Evaluation of the Foveon X3 sensor for astronomy

Anna-Lea Lesage, Matthias Schwarz
alesage@hs.uni-hamburg.de,
Hamburger Sternwarte

October 2009

Abstract

Foveon X3 is a new type of CMOS colour sensor. We present here an evaluation of this sensor for the detection of transit planets. Firstly, we determined the gain , the dark current and the read out noise of each layer. Then the sensor was used for observations of Tau Bootes. Finally half of the transit of HD 189733 b could be observed.

1 Introduction

The detection of exo-planet with the transit method relies on the observation of a diminution of the flux of the host star during the passage of the planet. This is visualised in time as a small dip in the light curve of the star. This dip represents usually a decrease of 1% to 3% of the magnitude of the star. Its detection is highly dependent of the stability of the detector, providing a constant flux for the star. However ground based observations are limited by the influence of the atmosphere. The latter induces two effects : seeing which blurs the image of the star, and scintillation producing variation of the apparent magnitude of the star. The seeing can be corrected through the utilisation of an adaptive optic. Yet the effect of scintillation have to be corrected by the observation of reference stars during the observation time.
The perturbation induced by the atmosphere are mostly wavelength independent. Thus, recording two identical images but at different wavelengths permit an identification of the wavelength independent effects.

In this article we present our evaluation of one new type of sensor for application in the astronomy, precisely the transit detection. The aims of the utilisation of the Foveon X3 sensor are developed in section 2. A brief characterisation are to be found in section 3, finally the observational results from the Hamburg Observatory are commented in section 4.

2 Aims

Foveon X3 is a new type of CMOS sensor used for colour imaging. Its structure is based on a superposition of three layers with same number of pixels. The layers are alternatively n- and p-doped providing three imbricated and independent pixels. Each layer produces an image at a different wavelength band (figure 1) due to the wavelength dependent absorption coefficient of the silicium substrate (Hubel (2005) and Hubel et al. (2004)). For each exposure, this sensor produces three overlapping images at different wavelengths.

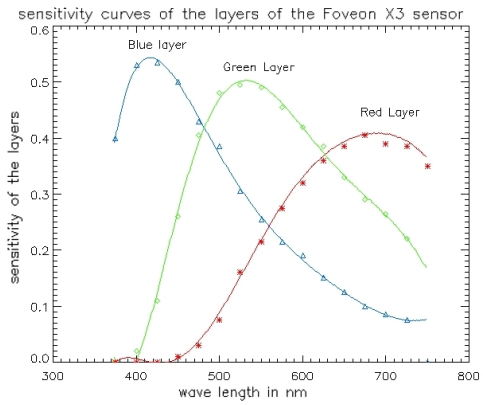

Figure 1: Sensitivity curves for each layer of the sensor (Hubel (2005))

2.1 Transit curve simulation parameters

The simulation of the transit is based on the following parameters : the transit duration is fixed on two hours, the depth of the transit dip is fixed on 3% of the nominal star intensity. Moreover the star is chosen to be Sun-like, hence its limb darkening is calculated from the formula given by Scheffler & Elsaesser (1990) for the Sun's limb darkening. The simulation of the transit is done with 220 data points, corresponding to one image per minute (figure 2). Finally the sensibility of each layer of the detector is then introduced into the model.

2.2 New transit profile

Most of the atmospheric effects on the light curve can be identified by comparison between the light curves of each layer. One layer is chosen as a reference. The light curves of the remaining layers are then divided by this reference light curve. This produces a new transit profile (figure 3).
In order to verify its possible use for the transit detection, the sensor had to be tested for stability and for identification of the possible noise sources. Thus it underwent a characterisation process and a observation campaign on the telescope.

3 Evaluation of the sensor

The sensor could only be found mounted inside the SD14 camera from Sigma. As an amateur photograph camera, it has inboard programs intended for images treatment before writing the images. We list here some of the actions produced by the camera's programs.

- Output file format : we used the code based on Dave Coffin's public domain (dcraw.c) for the conversion of the .X3F into .Fits which was already used by Hytti (2005)
- Dynamical range interpolation
- Dark noise reduction (see chapter 3.1).
- Limited exposure time : the camera cannot take images with an exposure time above 2 minutes.

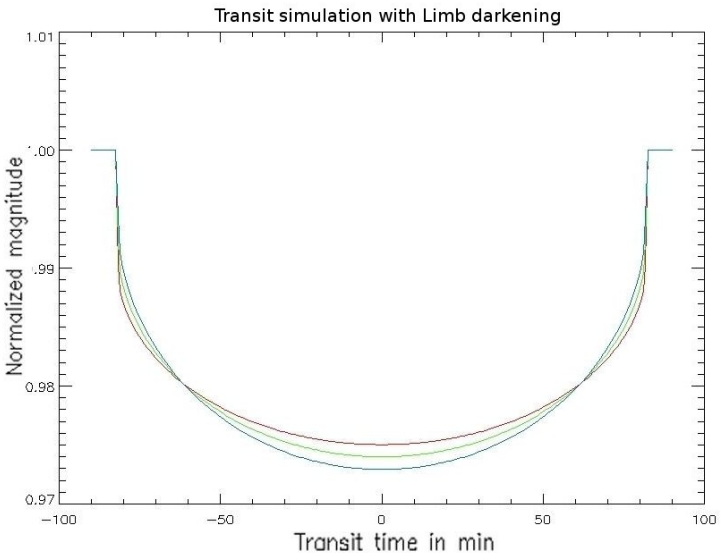

Figure 2: Transit profile including the effects of the limb-darkening of the star and the sensitivity curves of the sensor.

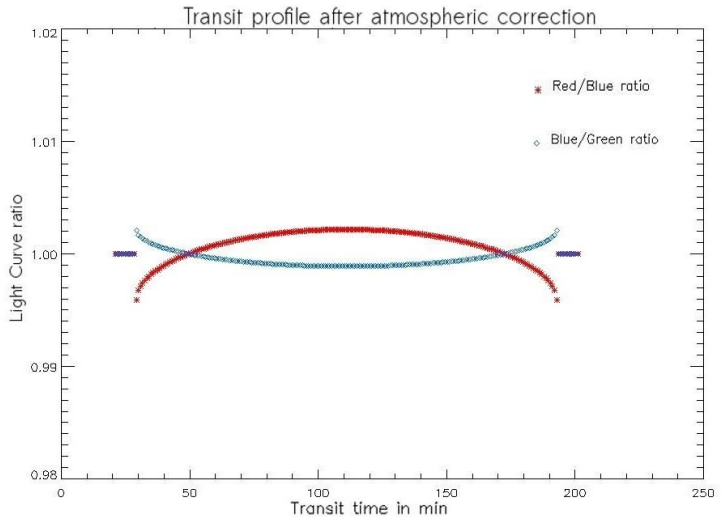

Figure 3: New transit profile by using the green layer as reference for the atmospheric correction.

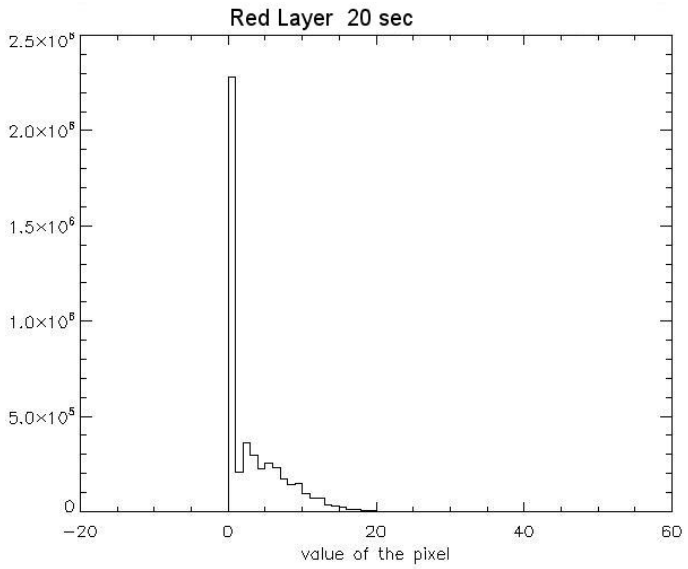

Figure 4: Histogram of a dark image taken with 20 sec exposure time

3.1 Dark Current

For two dark images taken with the camera, at very different exposure times, the histogram distributions present the same profile : a majority of pixel with a value of 0 ADU (figure 4). Moreover the reading time of an image is proportional with the exposure time. We conclude that the inboard noise reducing program of the camera operates by taking and subtracting a dark image for every image.
Due to this subtraction, the determination of the read out noise could not be performed as usual. Therefore, it was determined simultaneously with the gain.
Thermic energy inside the sensor creates electrons which are counted as signal when the reading of the sensor. The camera is not cooled so the sensor was tested here for a room temperature of 22°C. A set of 10 identical dark images were taken for increasing exposure time. The following assumption is taken : $\sigma_{d1} \simeq \sigma_{d2} \simeq \sigma_d$.
Resulting the determination of the dark current as : $\sigma_d = \frac{\sigma_{measured}}{\sqrt{2}}$

3.2 Gain and Read-Out Noise

The gain was calculated for each pixel. For an increasing exposure time, at constant illumination, 10 images were made, producing data cube of (2651,1768, 10) pixels. The mean value and the standard deviation for each pixel are calculated in the time dimension. The variance of each pixel is finally plotted against the mean value. The gain is calculated as the inverse of the slope of the fit (see figure 5). The Read-Out Noise is read on the curves as the intersection between the fitted curve and the y axis. Figure 6 represents the gain distribution for all the pixels of the green layer. The results of the characterisation can be found in table 1.

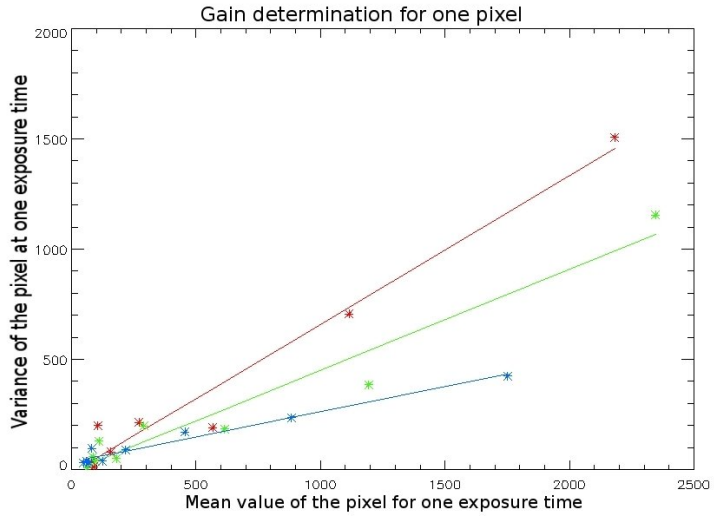

Figure 5: Determination of the gain

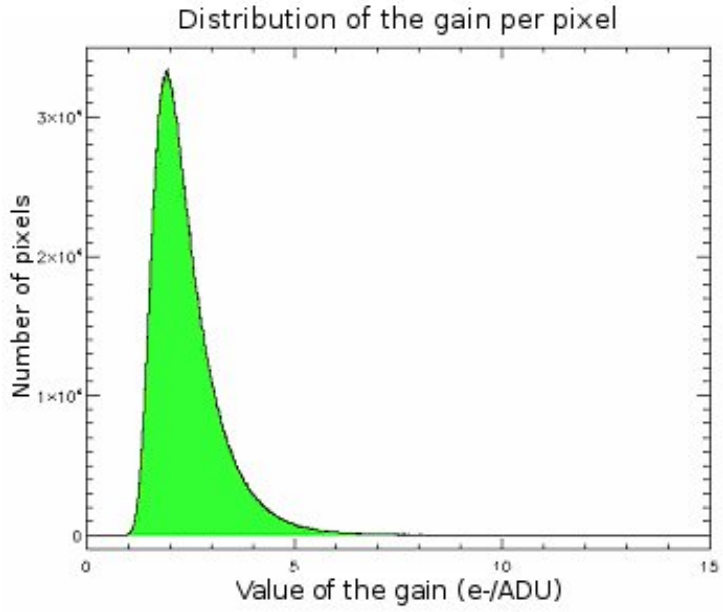

Figure 6: Gain distribution for the pixels of the green layer

Layer	Gain e^-/ADU	RON e^-	Dark Current e^-/pix/sec
Red	2.1 ±0.7	4.4 ±0.5	2.3 ± 0.1
Green	2.4 ±0.8	4.9 ±0.5	2.6 ± 0.1
Blue	3.7 ±1.6	7.4 ±1.1	3.9 ± 0.3

Table 1: Characterisation results of the sensor

4 Observations with Foveon X3

4.1 Observation of a bright star

The camera was mounted on the Oskar Lühning telescope of the Hamburg Observatory. As most of the known transit stars have magnitude of 7.5 or more, we have determined up to which star magnitude it is possible to observe with a Signal to Noise ratio higher than 5 for every layer. Above a magnitude of 9.25 the stars observed do not compelled the criteria.
The capability of the sensor for photometry observations was tested on Tau-Bootes. The images reduction was done for each layer with the DAOPHOT program APER on IDL. The three light curves present high resemblances : the red and the green one are perfectly overlapping, while the blue one follows the same profile (figure 7) . The green layer was chosen as reference layer for the correction of the wavelength dependent effects. Thus, the remaining light curves were divided by the reference. The final light curve ratio presents mostly variation which are inherent to the camera.

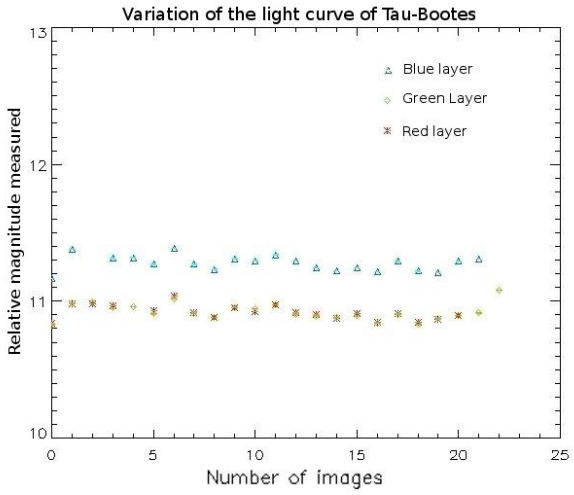

Figure 7: Variation of the light curve of Tau Bootes for each layer of the sensor.

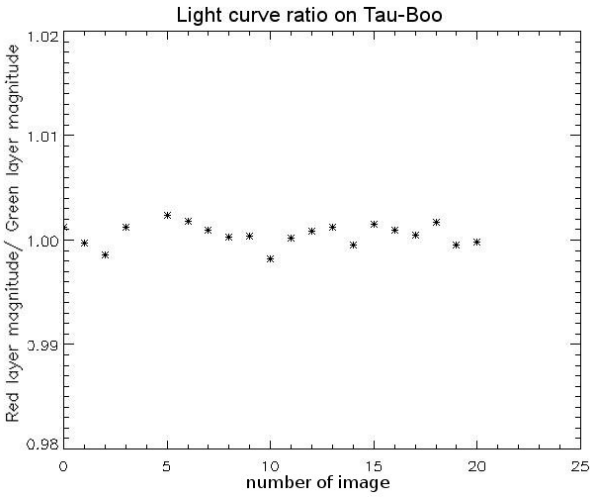

Figure 8: Variation of the ratio of the light curves of Tau Bootes with the green layer as reference

The standard deviation for the light curve ratio was estimated at 0.0016 magnitude with a signal to noise ratio of 17. We inserted this value of noise into our model for the new transit profile. For one observation per minute, the fit for the searched transit profile provided a goodness of fit factor χ^2 of 0.0005 despite the large noise level. The profile could still be retrieved for noise up to 0.025 magnitude for 222 data points.
Observations on transiting planets should confirm the use of this method for transit detection.

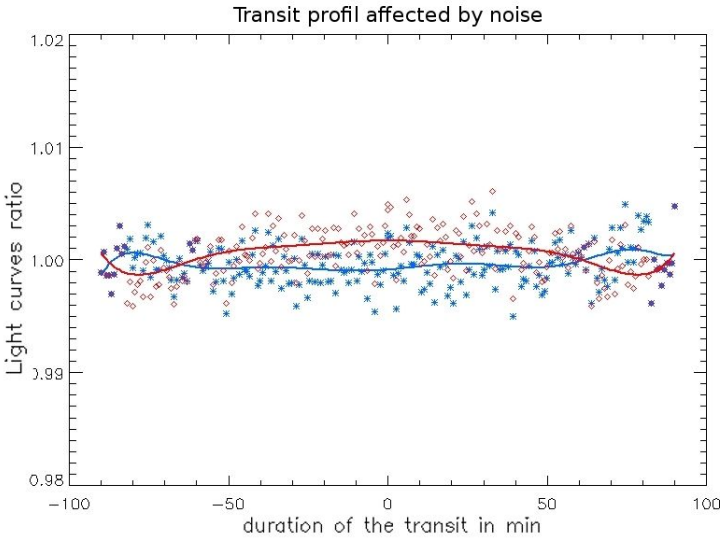

Figure 9: Simulation on the transit profile implemented with a random noise. The transit profile can still be recovered through an appropriated fit.

4.2 Observation of HD 189733

Observations were made on HD 189733 and HD 209458, two of the brightest stars with known transit planets. The observation of the transit of HD 209458 was not conclusive, due to weather condition. However the light curve of the transit of HD 189733 b show a slight decrease after 30 min (see figure 10). Only half of the transit was measured before dawn, yet a trend can clearly be identified. However, once the light curves were divided by a reference light curve, it is not possible to retrieve the new transit profile. The difference between the light curve due to the limb darkening of the star are too faint to be identified.
Further observations of these two stars should nevertheless be done.

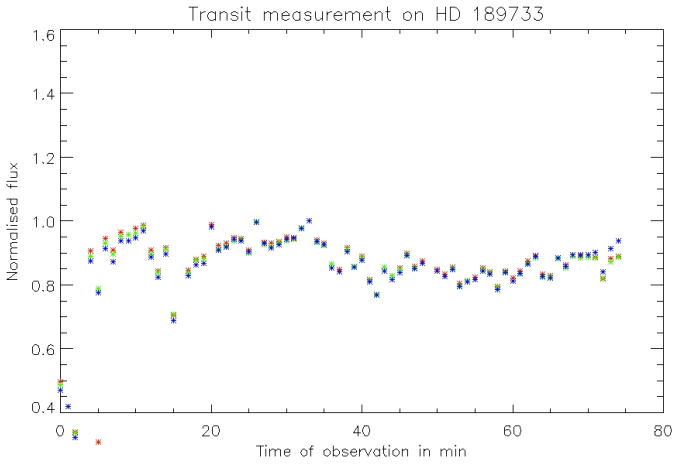

Figure 10: Light curves of HD 189733 during a transit

5 Conclusions

Due to the noise reduction program inside the camera, the images recorded with the sensor are not saturated with noise despite a relatively high exposure times. The dark current noise reduction also allows to skip the recording of the dark images during the observations. Yet for very faint stars, the image of the star could become more noisy than before subtraction.
The sensor has proved during observations that it can provide stable images for photometry. The transit profile can even be directly identified from the light curves recorded without any correction. However the observations made on the two brightest stars with transiting planets showed that the differences between the light curves recorded by the layers are too faint to permit a correction of the atmospheric effects. This is due to the mostly overlapping sensitivity curves of the sensor. Nonetheless the overlap can be reduced by using colour filters. Further observations would be needed to improve the observational capacity of this sensor.

References

Hubel, P. M. (2005), Foveon technology and the changing landscape of digital cameras, *in* 'Thirteenth IS&T Color Imaging Conference', Thirteenth IS&T Color Imaging Conference, pp. 314–317.

Hubel, P. M., Liu, J. & Guttosch, R. J. (2004), Spatial frequency response of color image sensors: Bayer color filters and Foveon X3, *in* M. M. Blouke, N. Sampat & R. J. Motta, eds, 'Society of Photo-Optical Instrumentation Engineers (SPIE) Conference Series', Vol. 5301 of *Presented at the Society of Photo-Optical Instrumentation Engineers (SPIE) Conference*, pp. 402–407.

Hytti, H. (2005), 'Characterization of digital image noise properties based on raw data', *Image Quality and System Performance III, SPIE*.

Scheffler, H. & Elsaesser, H. (1990), *Physik der Sterne und der Sonne*, BI Mannheim.